THEORY AND MEASUREMENT OF THE ELECTRON CLOUD EFFECT[#]

K. C. Harkay [+], Advanced Photon Source
Argonne National Laboratory, Argonne, IL 60439 USA

Abstract

Photoelectrons produced through the interaction of synchrotron radiation and the vacuum chamber walls can be accelerated by a charged particle beam, acquiring sufficient energy to produce secondary electrons (SEs) in collisions with the walls. If the secondary-electron yield (SEY) coefficient of the wall material is greater than one, a runaway condition can develop. In addition to the SEY, the degree of amplification depends on the beam intensity and temporal distribution. As the electron cloud builds up along a train of stored bunches, a transverse perturbation of the head bunch can be communicated to trailing bunches in a wakefield-like interaction with the cloud. The electron cloud effect is especially of concern for the high-intensity PEP-II (SLAC) and KEK B-factories and at the Large Hadron Collider (LHC) at CERN. An initiative was undertaken at the Advanced Photon Source (APS) storage ring to characterize the electron cloud in order to provide realistic limits on critical input parameters in the models and improve their predictive capabilities. An intensive research program was undertaken at CERN to address key issues relating to the LHC. After giving an overview, the recent theoretical and experimental results from the APS and the other laboratories will be discussed.

1 INTRODUCTION

Electron cloud (EC) effects involve the interaction between high-energy beams and low-energy electrons produced in the vacuum chamber. These interactions are essentially nonresonant in nature, unlike the well-known phenomenon of ion-trapping [1], widely observed in electron and anti-proton storage rings. A major contribution to the electron cloud in high-energy, multibunch lepton rings are photoemitted electrons (PE) produced through the collision of synchrotron radiation photons and the vacuum chamber walls. Ionization of the residual gas is a negligible source of electrons for typical vacuum pressures. The surface condition, material, and geometry of the vacuum chamber are important considerations in the photoelectron yield, Y, as is the photon energy and incident angle. The electron cloud distribution further depends on the photon reflectivity, R. The published Y, R data differ in some details [2][3]; other uncertainties in predicting EC effects lie in choosing realistic parameters for the photon energies and incidence angles. The most severe effects are expected in chambers without an antechamber, such as in the PEP-II interaction region [4]. Even with an antechamber to pass most of the high-energy photons, a storage ring chamber is typically designed with a number of absorbers to intercept photons to protect downstream surfaces such as flanges and ceramic chambers. The absorbers can serve as a dominant source of PE, as observed at the APS [5].

The photoelectrons can be accelerated by a charged particle beam, acquiring sufficient energy to produce secondary electrons in collisions with the walls. If the secondary-electron yield (SEY) coefficient of the wall material is greater than one, the runaway condition of beam-induced multipacting can develop. In addition to the SEY, the degree of amplification depends on the beam intensity and the temporal distribution. The former determines the incident electron energies and the latter determines whether a resonance condition is satisfied between the bunch spacing and the wall-to-wall time-of-flight of the electrons. Beam-induced multipacting was first observed 20 years ago in the Intersecting Storage Ring (ISR), at which time a fast pressure rise of an order of magnitude was seen due to electron-induced desorption [6]. Photoemission can be thus be important in ~TeV hadron machines such as the LHC, primarily because of multipacting effects and heating of the superconducting magnet liners [7]. To avoid multipacting, a minimum SEY, close to unity, is desired. Photon reflectivity (R) also plays a key role in determining the electron distribution in regions with a dipole field [8]. Uncertainties in calculating the minimum SEY and maximum R involve the assumed energy and angular distribution of the incident cloud electrons.

As the electron cloud builds up along a train of stored bunches, a wakefield of sufficient magnitude can be produced through the local perturbation of the cloud by transverse offsets of the leading bunches. The effective wakefield is short-ranged, but for a large bunch number, the oscillation amplitude in the tail of the train can grow exponentially. Also called the beam-photoelectron instability or “Ohmi” effect, ECI was first described by K. Ohmi (KEK) in 1995 [9] after experimental evidence for it was found at the KEK Photon Factory (PF) [10]. The possibility of ECI at the KEK-B lead to a collaboration between KEK and IHEP (China) to undertake experiments at BEPC, where results similar to those at PF were obtained and a detailed study of the dependence of the instability on machine parameters was made [11]. Although results from theoretical simulations are qualitatively consistent with these observations, the electrons had not been directly measured. The goal of studies at the APS was to directly characterize the electron cloud. The SEY for the oxidized Al chamber in the storage ring is >2 for incident electrons up to 1 keV [4][12], so a large effect was expected.

[#] Work supported by the U.S. Department of Energy, Office of Basic Energy Sciences, under Contract No. W-31-109-ENG-38.

[+] Email: harkay@aps.anl.gov

In this overview, the initial experimental evidence for electron cloud instabilities is reviewed, including relevant observations on phenomena involving trapped electrons. Recent analytical results, including refinements of the models, are presented. Recent experimental results from CERN, APS, PEP-II, and BEPC are then described. Table 1 gives the parameters for the machines discussed.

2 EXPERIMENTAL OBSERVATIONS

The most convincing evidence for ECI are similarities between theoretical predictions and experiments performed at the PF, BEPC, and CESR, which include positron vs. electron behavior, growth rate, effect of bunch spacing, and effect of bunch current on spectrum.

In machine experiments at PF [10] and BEPC [11], vertical coupled-bunch instabilities were observed with positrons and electrons, but with different instability thresholds and characters. For electrons, the threshold was higher, excitation of rf cavity HOMs were seen, and the betatron sideband spectrum was narrow. For positrons, the threshold was lower, no HOM signals were seen, and the sideband spectrum was broad. The threshold was not affected by the operation of the distributed ion pumps (DIPs). At the PF, the peaks of the betatron spectrum shifted with beam current, unlike what would be expected with a conventional coupling impedance. The instability was not completely suppressed with a bias voltage applied to the position monitors (clearing electrode), but could be overcome using octupoles. At the BEPC, a fit to the betatron spectrum shows the range of the wakefield to be 2-4 bunches. The instability was very sensitive to vertical chromaticity, emittance, bunch spacing, and rf frequency (horizontal orbit position), and weakly dependent on the energy. The damping effect of high chromaticity is thought to involve a combination of head-tail and Landau damping [9]. The instability threshold increased by a factor of 4 after increasing the bunch spacing by a factor of 2.

A horizontal coupled-bunch instability involving PE electrons trapped in the combined quadrupole electrostatic leakage field from the DIPs and bending magnet field was observed at CESR [13]. The transverse position of the beam modulates the trapped charge density, which in turn produces a time-dependent force on the beam, similar to ECI. Calculations show that the wakefield is long-range, but that SE are unimportant at the nominal bunch spacing (280 ns). No ECI-like effects were seen for spacings > 14 ns, but preliminary data at a 2-ns spacing shows a betatron sideband signature similar to PF and BEPC [14].

A broadly studied beam-electron interaction in a machine very different from these is the "e-p" instability at the Proton Storage Ring (PSR) at LANL [15]. Plans for very high-intensity proton drivers (>10^{14} protons/pulse) for the spallation neutron source and muon collider have generated renewed interest in understanding the e-p effect. Experiments indicate that coupled oscillations of low-energy electrons and beam protons develop when electrons are trapped in the beam potential well. Charge collected on electrodes when the beam becomes unstable is believed to have a contribution from beam-induced multipacting. The peak in the unstable frequency spectrum depends on the current and bunch length. Clearing electrodes have minimal effect on increasing the instability threshold. There is some recent evidence that an e-p instability has been observed at the CERN Proton Source [16].

Transverse coupling between bunches mediated by the free electrons in ECI is similar to the dynamics with free ions in the fast beam-ion instability (FBII), first proposed theoretically, and then observed at Pohang Light Source (PAL), Advanced Light Source (LBNL), and TRISTAN (KEK) [17]. FBII persists even with a gap much longer than is necessary to clear classically trapped ions.

3 THEORY/SIMULATION

The three major numerical models for electron cloud effects were developed by K. Ohmi at KEK [9], M. Furman and G. Lambertson at LBNL [4], and F. Zimmermann at SLAC [18], the latter further developed by O. Brüning at CERN [19]. Simulation studies are complemented by analytical work by S. Heifets at SLAC [20] and N. Dikansky at BINP [21]. The codes give qualitatively similar results. First, the electron cloud is established by synchrotron photons emitted by a train of bunches, the distribution balanced between production and absorption processes. In the range of 10-100 eV photon energy, for example, the normal incidence Y for Al ranges between 0.2 and 0.06 [2]. Both the yield and the photon reflectivity, R, increase

Table 1: Machine parameters

	PF	BEPC	CESR	APS	PEP-II	KEKB	LHC	PSR
E (GeV)	2.5	2.2	5.3	7	3.1/9*	3.5/8*	7000	0.8
max. # bunches, N	312	160	1281	1296	1658	5120	2835	1
min. bunch spac. (m)	0.6	1.5	0.6	0.85	1.26	0.59	7.5	–
I (max.) (mA)	300	20-30	300♣	100	2140/980	2600/1100	540	2×10^{13} p
photon critical E (keV)	4	2.3	3.7	19.5	4.8&	6&	0.044	–
chamber radius or semi-axes (h × w) (mm)	☒	29×60	25×45	21×42	25×45&	48&	22	50
chamber material	Al	Al	Al	Al	TiN,Cu,SS	Cu	Cu	SS

* LER (e+) / HER (e-) & LER only ♣ N = 27 ☒ not available

for smaller incident angles. The force of the beam on the electrons is then computed, and the electrons are allowed to drift between bunch passages. In the impulse approximation, the momentum kick of an electron at a radial position, r, is $\Delta p_e = 2m_e c r_e N_b / r$, where $r_e = 2.8\times10^{-13}$ cm is the classical electron radius and N_b is the number of beam particles. For better accuracy in the models, the beam is sliced longitudinally and the force on the electrons is computed for each slice. Space charge is included in the calculations, as is the contribution by the image charges on the wall. When an electron reaches a wall, SE are generated using the appropriate SEY coefficients, given the electron energy and incident angle [12].

To calculate coupled-bunch effects, the first bunch is displaced transversely, which drags the electron cloud with it. The following bunch feels a kick due to the potential of the offset cloud, perturbing the cloud further, and so on. The forces are either represented by an effective wakefield or calculated on a finite-element grid. The instability growth rates of the transverse, coherent, multibunch modes are then computed in the usual way [22].

The greatest variations in the cloud saturation levels and growth rates predicted in the codes involve the assumptions made in the electron production processes and the presence of an external magnetic field. The EC buildup is limited by space charge. The distribution in a field-free region is more uniform than in a dipole field, where the electrons are confined to move in tight vertical helices. The main consequence is the severe suppression of the horizontal component of the momentum transferred to the cloud electrons [4]. In this case, the electrons near the beam orbit are produced by photons scattered from the mid-plane to the upper and lower chamber surfaces. Given a large SEY, even electrons produced by ionization of the residual gas by the beam are sufficient to start a chain reaction. For PEP-II, it was found that coating the Al chamber with TiN, thereby lowering the SEY, reduced the instability growth time by a factor of ~20-40. The SEY for oxidized Al is >2 for primary electrons up to 1 keV, while for Ti, it is <1 [4][12]. This result is important in the case of LHC, also. Calculations indicated that depending on assumptions about Y, SEY, and R, the EC-induced heat load on the beam liner could far exceed the cryogenic budget of 1 W/m. As a result, an intensive research program at CERN to measure the relevant physical quantities, validate the theoretical estimates, and propose remedies has been initiated [7][23]. A minimum SEY of 1.3 was defined to prevent multipacting [8][19].

The buildup of the electron cloud depends on so many factors that it is not obvious that simple scaling rules can be found to apply the results from one machine to another [4]. The PE alone may be sufficient to cause a beam instablity, as is likely to be the case in PF, KEKB, and BEPC. Even if the SEY is high, all the secondaries are lost if the bunch spacing is large; then only the PE are important. At a smaller bunch spacing, the SE can dominate for large SEY. In this case, primary PE may no longer be important, and even ionization electrons can lead to blowup, as in the ISR [6].

In the case of coupled-bunch instabilities, the range of the wakefield sets an upper limit to the bunch spacing at which ECI is important. This appears to be the case at both BEPC, where the ECI threshold increased for twice the bunch spacing, and at CESR, where an EC-like betatron spectrum was seen only when the bunch spacing was < 14 ns. The range of the wakefield is determined by both the average electron kinetic energy and by their density distribution. But if secondary emission and hence multipacting are unimportant, then the range of the wakefield is critically dependent only on their kinetic energy [24]. Therefore, while electron cloud effects are essentially nonresonant in nature, beam-induced multipacting effects can be important. It is observed that both multipacting and ECI could be important in both positively and negatively charged beams [5][6][9][24].

4 RECENT MEASUREMENTS

Of particular interest for recent measurements is to provide realistic limits on critical input parameters in the models to improve their predictive power. For example, a better knowledge of the fraction of photons diffused away from the forward direction and of the secondary electron energy distribution is required to understand the beam-induced multipacting heat load for LHC [7]. Comparison of independent codes (Furman and Zimmermann) has led to a convergence in the results at the 20% level for LHC simulations.

4.1 CERN

Photon irradiation tests were performed using an existing Electron-Positron Accelerator beamline at CERN to study the photoelectron yield, Y, and photon reflectivity, R [8]. A 4.2-m-long SS test chamber was irradiated at a grazing incidence (11 mrad) by 45 eV and 194 eV photons. The Cu liners inserted were of varying surface preparation and roughnesses, including a sawtooth structure with 0.5-mm steps quasi-perpendicular to the incident photons. Both Y and the forward scattering R were smallest for the sawtooth surface. Surface treatments such as TiN deposition, air oxidation, electron bombardment, and standard *in situ* baking are considered options for reducing the SEY, although the latter is rather difficult in the cold arcs of LHC. The use of a ribbed chamber wall for the purpose of shadowing top and bottom faces of the beam screen from reflected photons is being investigated [25]. The coupling impedance of such a surface is also under investigation.

Multipacting tests were performed using a resonant coaxial cavity [26]. A peak rf voltage of ~4.5 kV at 500 MHz could be achieved between the inner and outer conductor; the minimum expected voltage required for the multipacting threshold is 1.5 kV. Varying the rf voltage is equivalent to changing the beam current (i.e., accelerating potential). An amplitude-modulated signal was used to

detect the onset and rise time of multipacting with and without a dipole field while varying a solenoidal magnetic field. It was found that a 50-G solenoidal field can lower the secondary yield in the drift spaces, but it is ineffective with a strong dipole field. It is hoped that these data may provide direct information on SEY and, possibly, the energy distribution of the SE. A sharp decrease in the multipacting threshold was observed when the dipole field has an intensity such that the electron cyclotron frequency is equal to the resonant frequency of the coaxial cavity.

4.2 APS

To measure the properties of the electron cloud, a special 5-m vacuum chamber, equipped with rudimentary electron energy analyzers, beam position monitors (BPMs), and targets, was installed in a field-free region in the APS storage ring [5]. Two detectors are shown mounted on a standard-aperture vacuum chamber in Figure 1. A removable, water-cooled target is shown inserted in the antechamber channel. Data were collected by measuring the collector current with a picoammeter as a function of bias applied to the retarding grid.

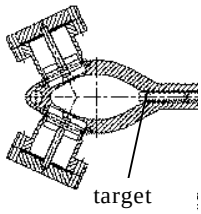

Figure 1: Cross-section schematic showing mounting of detectors.

The dependence of the detector current, normalized to the total positron beam current, on the detector location is seen in Fig. 2. In this example, 20 mA are stored in 10 bunches spaced at either 128 (0.36 μs) or 7 rf buckets (20 ns). As expected, a downstream Cu end absorber (EA6) is the primary source of electrons, dominating the signal at the detectors < 0.3 m away. The normalized electron current at the larger spacing is identical to that with a single bunch; therefore, this current vs. voltage (I-V) signature is believed to be determined mostly by the PE.

A **dramatic** amplification of the signal is observed at the 7-bucket bunch spacing. This can be attributed to the SE contribution. Detectors >1.4 m from EA6 show a higher amplification, which we speculate comes from multiple scattering of electrons originating from the absorber. A scan in the bunch spacing (10 bunches total) gave a peak in the normalized electron current at a spacing between 8-10 buckets. There is additional factor of 2.6 amplification in the normalized signal when the beam current increases from 10 to 20 mA. These data give evidence of a beam-induced multipacting effect [6]; the bunch spacing at the peak current equals the wall-to-wall time-of-flight in the vertical direction of electrons with an average energy of 8-12 eV.

The electron energy distribution is extracted from the derivative of the I-V curves and is dominated by low- energy electrons. The bunch spacing affects the shape of the high-energy tail, giving a longer tail for the multipacting conditions.

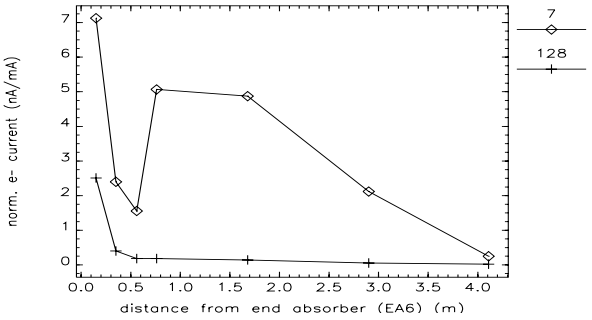

Figure 2: Total, normalized electron current per detector vs. distance from downstream end absorber as a function of bunch spacing (10 bunches, 20 mA).

The measured buildup of the electron cloud was most pronounced at the 7-bucket spacing, and the most dramatic increases occurred for detectors farthest from EA6. Figure 3 shows the normalized detector current 3 m from EA6 for bunch trains of varying length, with 1-2 mA/bunch. The total amplification at 2 mA/bunch is a factor of 360 in normalized current. A local pressure rise of a factor of 20 was observed for these conditions, indicative of enhanced desorption induced by the secondary electrons, and giving independent evidence of the multipacting effect [6]. A saturation effect is observed after a certain number of bunches, beyond which the increases becomes linear.

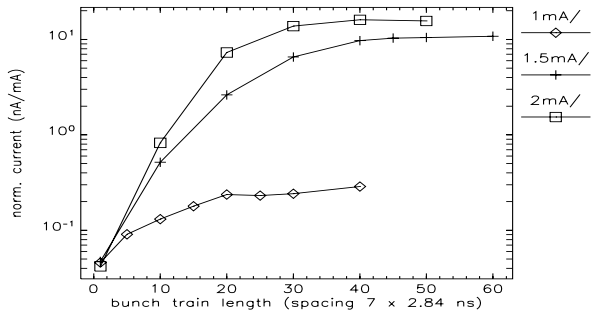

Figure 3: Amplification of EC over bunch trains.

More modest amplifications were seen for long electron bunch trains, but at a spacing of 11 buckets. The buildup of the electron cloud was also observed over long trains of electron bunches, with a similar saturation effect. Preliminary results with targets of different materials show a SE reduction for Cu or TiN surfaces compared to oxidized Al.

4.3 PEP-II LER

An initial search for electron cloud effects was made, with no clear evidence of ECI [27]. There is, however, fairly clear evidence for beam-induced multipacting, accompanied by a significant pressure rise with 500-1000 bunches and currents above 1 mA/bunch [24].

4.4 BEPC

Further refinements of ECI rise times have been made with time-domain measurements using a single-pass BPM

system [29]. The measured value of ~6 ms compares well with the predicted value of 3 ms.

5 DISCUSSION

Independent experimental results at CERN, APS, and PEP-II regarding electron cloud effects are beginning to converge. Evidence of beam-induced multipacting at APS with long trains of bunches spaced at 20 ns and 2 mA/bunch was accompanied by a significant local pressure rise. The pressure rise with 1 mA/bunch was not significant. Evidence of multipacting at PEP-II shows a very similar bunch-current-dependent pressure rise effect, with a threshold at 1 mA/bunch. The vertical aperture and 20-ns bunch spacing at APS are nearly the same as the LHC aperture and bunch spacing, for which calculations predict that multipacting conditions are satisfied. Even though the maximum energy of photoelectrons impinging on the walls by the impulse approximation are very different, 200 eV at LHC vs. 10 eV at APS, the peak of the SE energy distribution of ~5 eV is nearly independent of material and incident electron energy [12].

Electron bombardment of the chamber surface was measured in bench tests to lower the SEY. At SLAC, a 25% reduction was seen after a dose of ~10^{18} e/cm^2 (15 A-h equivalent in PEP-II) [4], and at CERN a dose of 10^{-3} C/cm^2 reduced the Cu SEY to below 1.3, the critical value for multipacting [28]. Data with the APS Al chambers show that the SE-dominated signal was reduced by 45% after 62 A-h of stored beam.

Saturation effects due to space charge and the dependence on the bunch current and other critical parameters (Y, R, SEY) have been studied in simulations and analytical work [4][18][20][21]. A bunch-current-dependent saturation effect was measured with long bunch trains at the APS (Fig. 3); these data may provide a benchmark for calculations of the equilibrium electron cloud density. Comparisons of these and other APS data with simulations are planned, with the view of perhaps developing an empirical model for realistic chamber geometries.

Remaining questions include: how far can active damping and passive control (necessary in LHC) raise the threshold for electron cloud effects? A solenoidal B-field is only effective in field-free regions [26]. Clearing electrodes have not shown promise as being effective (PF, PSR, etc). Quantitative measurements of the growth rate at BEPC [29] suggest that a feedback system may be effective. There is a need for a more quantitative theory. For example, only vertical blowup is seen in ECI, while the present theory does not favor either plane. ECI is not a resonant phenomenon *per se*, but beam-induced multipacting appears to be an important effect in the buildup of the electron cloud. What is the role of other resonant effects, such as when the EC cyclotron frequency in the dipoles equals the betatron frequency or the resonant frequency of a structure in the vacuum chamber? Calculations have been made of the influence of quadrupoles on the SEY [19]. However, electron trapping in quadrupoles, such as occurs in the DIP-induced instability at CESR [13], may be important. A kinetic description of the e-p effect as an electron-ion two-stream instability may be a promising theoretical approach for understanding the broader array of electron cloud effects [30].

6 ACKNOWLEGEMENTS

The author would like to thank R. Rosenberg, J. Galayda, S. Milton, L. Teng, M. Furman, S. Heifets, Z. Guo, O. Brüning, and J. Rogers for their generous assistance.

7 REFERENCES

[1] Y. Baconnier and G. Brianti, CERN Report No. CERN/SPS/80-2 (DI) (1980)

[2] O. Gröbner et al., J. Vac. Sci. Technol. A7, 223 (1989); R. B. Cairns and J. A. R. Samson, J. Opt. Soc. 56, 1568 (1966); B. L. Henke, J. P. Knauer, K. Premaratne, J. Appl. Phys. 52 (3), 1509 (1981); R. H. Day et al., J. Appl. Phys. 52 (11), 6965 (1981)

[3] B.L. Henke, E.M. Gullikson, J.C. Davis, Center for X-ray Optics, Web page: www-cxro.lbl.gov/optical_constants/mirror2.html

[4] M. Furman, Proc. of MBI97, KEK Proc. 97-17, 170 and 234 (1997) and Proc. of 1997 PAC, 1617 (1998)

[5] K. C. Harkay and R. A. Rosenberg, "Measurements of the Electron Cloud in the APS Storage Ring," these proceedings

[6] O. Gröbner, Proc. of 10th Int'l Conf. on High Energy Accel., Protvino, 277 (1977)

[7] V. Baglin et al., Proc. of 1998 EPAC, 359 (1998)

[8] V. Baglin et al., Proc. of 1998 EPAC, 2169 (1998)

[9] K. Ohmi, Phys. Rev. Lett. 75, 1526 (1995); Proc. of 1997 PAC, 1667 (1998); and KEK Report 97-7 or IHEP/BEPC/AP/97-09

[10] M. Izawa, Y. Sato, T. Toyomasu, Phys. Rev. Lett. 74, 5044 (1995)

[11] Z. Y. Guo et al., Proc. of 1997 PAC, 1566 (1998) and Proc. of 1998 EPAC, 957 (1998)

[12] W. H. Kohl, Handbook of Materials and Techniques for Vacuum Devices, AIP Press (1995); Seiler, Phys. 54 (11) (1983)

[13] T. Holmquist and J. T. Rogers, Phys. Rev. Lett. 79, 3186 (1997)

[14] J. T. Rogers, KEK Proc. 97-17, 42 (Dec. 1997)

[15] M. A. Plum et al., Proc. of 1997 PAC, 1611 (1998)

[16] B. Zotter, in private communication from R. Cappi (1998)

[17] T. O. Raubenheimer and F. Zimmermann, Phys. Rev. E 52, 5487 (1995); J. Y. Huang et al., Phys. Rev. Lett. 81, 4388 (1998); J. Byrd et al., Proc. of 1997 PAC, 1563 (1998); H. Fukuma et al., Proc. of 1997 PAC, 1596 (1998)

[18] F. Zimmermann, SLAC-PUB-7425 (1997) and Proc. of MBI97, KEK Proc. 97-17, 221 (1997).

[19] O. Brüning, Proc. of 1998 EPAC, 332 (1998)

[20] S. Heifets, Proc. of CEIBA95, KEK Proc. 96-6 (1996)

[21] A. V. Burov, N. S. Dikansky, KEK Proc. 97-17, 200 (1997)

[22] A. W. Chao, Physics of Collective Beam Instabilities in High Energy Accelerators, Wiley (1993)

[23] F. Ruggiero, "Electron Cloud in the LHC" Web page: wwwslap.cern.ch/collective/electron-cloud/electron- cloud.html

[24] M. Furman, private communication (1999)

[25] O. Brüning et al., "Electron Cloud and Beam Scrubbing in the LHC," these proceedings

[26] O. Brüning et al., Proc. of 1998 EPAC, 356 (1998)

[27] M. Furman et al., "Search for the Electron-Cloud Effect in PEP-II," these proceedings

[28] O. Brüning, private communication (1999)

[29] Z. Y. Guo et al., "Recent Studies on Beam-Photoelectron Instability in BEPC," these proceedings

[30] R. C. Davidson et al., "Kinetic Description of Electron-Proton Instability in High-Energy Linacs and Storage Rings," these proc.